

Cite this article as: Chen Yumei, Liu Quanzhen, Liu Anguo, et al. Twinning Assisted Dynamic Recrystallization and Related Microstructure Evolution During Large Strain Rolling of Mg-3Y Alloy[J]. Rare Metal Materials and Engineering, 2023, 52(06): 2068-2074.

ARTICLE

Twinning Assisted Dynamic Recrystallization and Related Microstructure Evolution During Large Strain Rolling of Mg-3Y Alloy

Chen Yumei, Liu Quanzhen, Liu Anguo, Hou Xiuli

School of Materials Science and Engineering, Jiangsu University, Zhenjiang 212013, China

Abstract: The Mg-3Y (wt%) alloy sheet was fabricated by pre-extrusion and subsequent single-pass large strain hot rolling process. The influences of different twinning types on dynamic recrystallization (DRX) and grain structure evolution during large strain hot rolling were investigated. Results show that the alloy undergoes nearly complete DRX during pre-extrusion processing under a low extrusion ratio of 8:1. During subsequent large strain hot rolling processing, deformation twinning, especially the $\{10\bar{1}1\}$ compression and $\{10\bar{1}1\}$ - $\{10\bar{1}2\}$ double twinning, plays an important role in plastic strain accommodation. Moreover, the compression twin and double twin assisted DRX occurs extensively within the grains, and the recrystallization region is extended from the twin interior towards non-twinned regions, greatly relieving the internal stress. Both of processes above promote the formability of the alloy during large strain hot rolling processing.

Key words: magnesium alloy; rare earth; large strain rolling; twinning; dynamic recrystallization

As the lightest metallic structural materials, magnesium and its alloys have become the competitive candidates in automotive and aerospace industries for the object of energy conservation and environmental protection^[1-3]. However, the hexagonal close-packed (hcp) crystal structure induces low ductility and unsatisfactory formability, which are still key factors limiting their practical application; the strong crystallographic texture formed during plastic forming processing also severely restricts further component manufacturing^[4-6]. Thus, the microstructure refinement and texture control have become the key topics in magnesium strengthening and toughening^[5,7]. Alloying magnesium with rare earth (RE) elements has been proved to be an effective way to improve both the strength and toughness of magnesium alloys, especially the exceptional texture weakening effect of RE additions in wrought magnesium products^[8-10]. Consequently, there is a great potential to develop high performance magnesium alloys with RE alloying and a combination of appropriate plastic forming processing.

Up to now, many innovative plastic forming techniques

have been developed, such as equal channel angular pressing (ECAP)^[11-12], spiral equal channel angular extrusion (SP-ECAE)^[13], high pressure torsion^[14], and accumulative roll bonding^[15]. All of them show great efficiency in microstructure refining and texture tailoring of magnesium alloys. Compared with these complex severe plastic forming techniques, hot rolling processing with plausible technological improvements, such as differential speed rolling^[16], high strain rate rolling^[17] and large strain rolling^[18-19], have become convenient and effective methods to greatly refine microstructures. Among them, large strain rolling is a convenient plastic forming method for high performance magnesium alloy sheets. Under the large strain rolling of magnesium alloys, deformation twinning is an essential deformation mechanism to relieve local stress concentration (the initial microstructure with ultra-fine grains is an exception), such as $\{10\bar{1}2\}$ extension twinning and $\{10\bar{1}1\}$ compression twinning which are commonly observed twinning models in magnesium and its alloys. The critical resolved shear stress to trigger $\{10\bar{1}2\}$ extension twinning is

Received date: January 21, 2023

Foundation item: National Natural Science Foundation of China (21403092); Natural Science Fund for Colleges and Universities in Jiangsu Province (17KJB430008)
Corresponding author: Hou Xiuli, Ph. D., Associate Professor, School of Materials Science and Engineering, Jiangsu University, Zhenjiang 212013, P. R. China, Tel: 0086-511-88797887, E-mail: houxiuli@ujs.edu.cn

Copyright © 2023, Northwest Institute for Nonferrous Metal Research. Published by Science Press. All rights reserved.

relatively low, ~ 12 MPa^[20], and thus these twins can quickly nucleate and propagate. Yet the extension twin boundaries can migrate swiftly, and the lattices undergone twinning will be set in hard orientation for basal slip^[21], it is of great importance to restrict the growth of extension twins. While $\{10\bar{1}1\}$ compression twins usually nucleate at a relatively higher strain or strain rate^[22-23], and once these twins are formed, they are immediately transformed into $\{10\bar{1}1\}$ - $\{10\bar{1}2\}$ double twins. The lattices either in compression twins or double twins are rotated in favorable orientations for basal slip, so the intense dislocation slips in twinned lattices can effectively release local stress concentration, but the strain incompatibility may be induced at the interface of twin boundaries if the surrounding matrix cannot activate sufficient dislocation slips^[24-25]. Consequently, the deformation twinning related microstructure evolution plays a critical role in the subsequent deformation behavior of the alloy. In practice, either twinning induced micro-cracking and prefailure due to local stress concentration^[24], or twinning assisted plasticity through the introduction of twin-twin network^[26] and twinning triggered dynamic recrystallization^[22-23] have been observed. Therefore, a detailed investigation on deformation twinning associated deformation mechanisms and microstructure evolution is necessary to solve the controversy.

In this study, the Mg-3Y (wt%) alloy was subjected to pre-extrusion and subsequent single-pass large strain hot rolling process with a thickness reduction of 50%, and then the alloy sheet was quenched immediately in order to obtain a completely as-deformed state. Optical microscopy (OM), electron backscatter diffraction (EBSD), transmission Kikuchi diffraction (TKD) and transmission electron microscopy (TEM) were used to study the twinning behavior and associated microstructure evolution after plastic forming processing and to discuss the related deformation mechanisms.

1 Experiment

The as-received material used in this study was a Mg-3Y (wt%) as-cast alloy ingot. Then the as-cast ingot was subjected to solution heat treatment at 520 °C for 12 h, followed by hot water quenching at about 60 °C. In order to get a better plastic forming ability during the subsequent rolling process, the solution heat treated ingot was pre-extruded with a low extrusion ratio of 8:1. The extrusion processing was carried out at 380 °C with a ram rate of 1 mm/s, and the obtained alloy sheet possessed cross dimensions of 80 mm×12 mm. After that, the alloy sheet was single-pass rolled at the temperature of 350 °C with the thickness reduction of 50%, and then the as-rolled sheet was immediately quenched by hot water (~ 60 °C) so as to preserve the as-deformed structure. The rolling rate was 20 mm/s and the extrusion direction was parallel to the rolling direction.

For microstructural observations, specimens were taken from the mid-layer of the pre-extruded/as-rolled alloy sheets using Struers Accutom 50. Optical microstructure observation was performed on the Olympus GX71. Twins and dynamic recrystallization in the as-rolled alloy were characterized by

EBSD and TKD analysis using high-resolution field emission scanning electron microscope (Zeiss Ultra Plus) equipped with an EBSD system (Oxford Instruments Aztec 2.0), operated at 30 kV. The corresponding data was analyzed by Channel 5 software. The more detailed characterization of twins, dislocations and dynamic recrystallized grains was accomplished by TEM (JEOL JEM-2100) observation, and the data was analyzed by Gatan Microscopy Suite. The specimens for OM and EBSD analysis were prepared by mechanical polishing and light etching in a polishing suspension at the last step. Foils for SEM-TKD and TEM observations were thinned to perforation with a precision ion polishing system, and cleaned in advance by Gatan 950 Solarus Advanced Plasma System before observation.

2 Results and Discussion

2.1 As-deformed microstructure and twin variants

Fig. 1a shows the EBSD inverse pole figure (IPF) map of pre-extruded alloy, which exhibits an equiaxed grain structure with the average grain size of 45 μm , indicating a nearly complete dynamic recrystallization (DRX) during the extrusion processing; yet some low angle grain boundaries are detected. Furthermore, some $\{10\bar{1}2\}$ extension twins are also observed in some grains, as presented in the image quality map (Kikuchi band contrast) in Fig. 1b. The micro-texture (Fig. 1c) of the as-extruded alloy shows a weak non-basal texture with the tilted basal poles apart from the center of $\{0001\}$ pole figure, i. e., the normal direction of the alloy sheet, which is common for rare earth containing magnesium wrought alloy sheets.

For the as-rolled alloy, a complex microstructure with severely deformed original grains and extensive parallel narrow bands across the deformed grains are observed, as indicated in Fig. 2a and 2b. Most of the narrow bands are kinked due to intense plastic deformation, and some bands intersect with each other. Moreover, some areas cannot be clearly detected and the interior of narrow bands may have undergone dynamic recrystallization, which needs to be confirmed by further observation. The physical nature of these parallel narrow bands should be clarified firstly.

Fig. 3 provides the EBSD IPF map (Fig. 3a) and corresponding image quality map (Kikuchi band contrast, Fig. 3b) of the as-rolled alloy. Some key information is obtained from the maps. Firstly, most of the narrow bands are detected to be $\{10\bar{1}1\}$ - $\{10\bar{1}2\}$ double twins (Fig. 3b), consistent with the reported investigations that compression twins (usually transforming into double twins) are usually triggered at higher strain or strain rate^[22-23]. Secondly, the interior of double twins undergoes dynamic recrystallization. As mentioned above, some ultra-fine grains form in the twinned region, so the indexed boundaries of twin lamellae are scattered. Besides the twinned region, dynamically recrystallized fine grains also nucleate in other regions of the matrix, as indicated by circles in Fig. 3. Finally, besides the dominated double twins, some $\{10\bar{1}2\}$ extension twins are

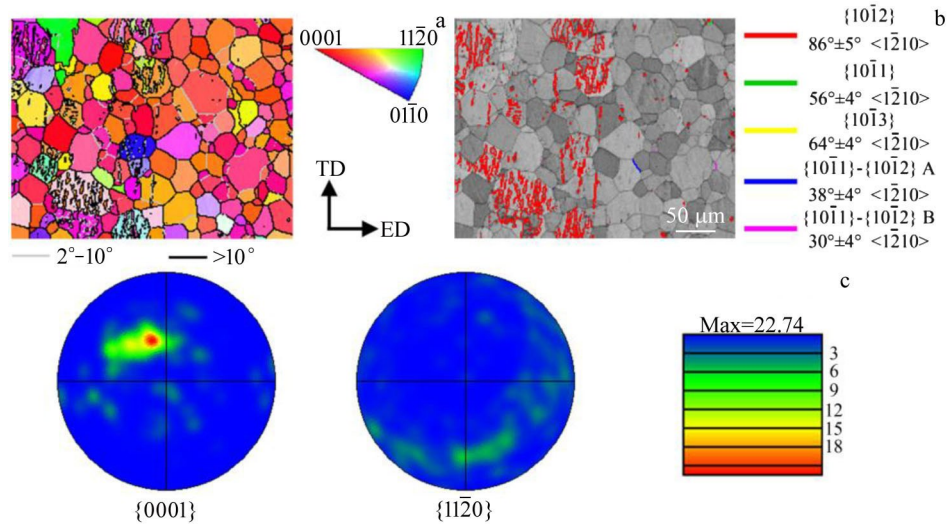


Fig.1 EBSD IPF map (a) and corresponding Kikuchi band contrast map (b), and {0001} and {1120} pole figures (c) of the as-extruded alloy

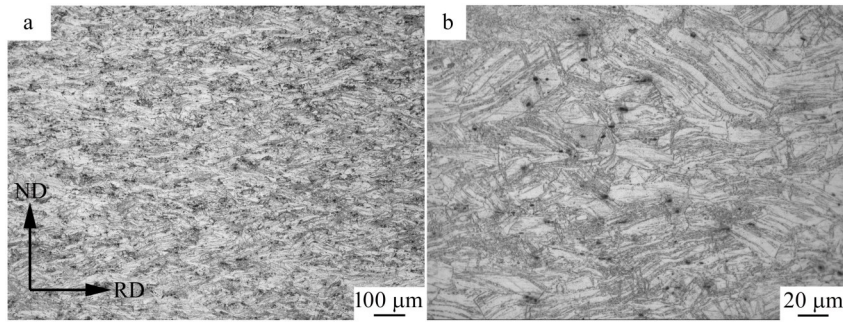


Fig.2 Optical micrographs of the as-rolled alloy

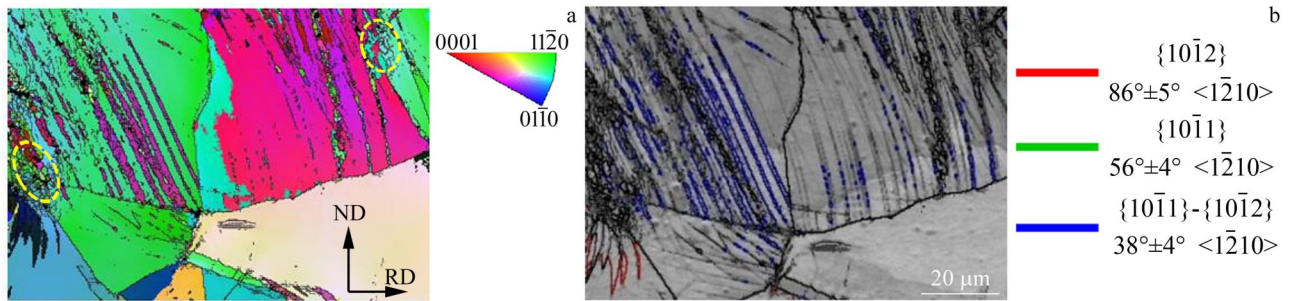


Fig.3 EBSD IPF map (a) and corresponding Kikuchi band contrast map (b) of the as-rolled alloy

detected, these crescent moon-like twins are not isolated but form some clusters. Because of the hard orientation for basal slips in the twinned lattices of extension twins^[21], there is no sign of dynamic recrystallization inside them. Overall, it can be inferred from Fig.2 and Fig.3 that during the large strain hot rolling processing, deformation twinning, especially the compression and double twinning, plays an important role in plastic strain accommodation. The subsequent dynamic recrystallization further consumes plastic strain energy, relieving the internal stresses. Both of them promote the formability of the alloy during large strain hot rolling processing.

2.2 Role of deformation twinning in microstructure evolution

To investigate the details of microstructure evolution and related deformation mechanisms, transmission Kikuchi diffraction (TKD) was further performed on the as-deformed alloy, as indicated in Fig.4 and Fig.5. Various twin types as well as different variants of {1011} - {1012} double twin are distinguished at the nano-scale. It can be seen that dynamic recrystallization in the deformed alloy is a complex process associated with the interactions between deformation twinning and dislocation slips.

Fig.4 represents a typical area with crossed narrow bands in which dynamic recrystallization has taken place, and moreover, the observed area passes across two grains. The IPF map (Fig.4a) and corresponding band contrast map (Fig.4b) reveal that, besides twinning induced band-like deformation structure, there are also many deformation kinking bands produced by dislocation slips, and these thin bands possess a low angle grain boundary with respect to the matrix (as indicated by black arrows). For the twinning induced bands, the boundaries of these bands are more complex at the nano-scale. Such as the horizontal bands' boundaries, besides the commonly observed A type $\{10\bar{1}1\}$ - $\{10\bar{1}2\}$ double twin boundaries, the B type double twin boundaries are also observed, as well as the non-transformed $\{10\bar{1}1\}$ twin boundaries and $\{10\bar{1}3\}$ twin boundaries. It has been reported that $\{10\bar{1}1\}$ and $\{10\bar{1}3\}$ compression twins usually co-exist^[27]. This observation explains the scattered $\{10\bar{1}1\}$ - $\{10\bar{1}2\}$ double twin boundaries observed in the EBSD maps of Fig.3 from another aspect. Inside the bands, except the dynamically recrystallized grain/sub-grain boundaries, there are also secondary extension twin boundaries which are bounded at the traces along the thickness of the double twin segments, as indicated in Fig.4b. It is clear that the secondary twinning process and dynamic recrystallization proceed nearly simultaneously. Either the twinned regions in the $\{10\bar{1}1\}$ compression twin or $\{10\bar{1}1\}$ - $\{10\bar{1}2\}$ double twin have been rotated to favor basal dislocation slips. The kernel average misorientation (KAM) map is presented in Fig.4c, which can reflect the distribution of dislocation density in different regions, further certifying this fact. However, dislocation slips or dynamic recrystallization within the twin are limited for the uniform plastic deformation during hot rolling processing. Many investigations have ascribed $\{10\bar{1}1\}$ compression twin

or $\{10\bar{1}1\}$ - $\{10\bar{1}2\}$ double twin associated pre-failure to the absence of coordinated plastic strain accommodation mechanism inside and outside the twins^[24-25]. In Fig.4a, it is found that sub-grains produced by dislocation rearrangement nucleate near the band boundaries in the non-twinned regions (as indicated by black arrows), and the KAM map also reveals that the network like structure caused by dislocation rearrangement extends from the band and grain boundaries towards surrounding regions.

As for the observations shown in optical (Fig.2) and EBSD (Fig.3 and Fig.4) micrographs, besides dynamic recrystallization occurring within the twinning associated band structure, fine grains also nucleate in other regions of the matrix. Fig.5 shows an area possessing different clusters of fine gains or sub-grains within one grain. Interestingly, these clusters of dynamically recrystallized fine gains or sub-grains still show an intense interaction between dislocation slips and twinning deformation as observed in Fig.4. In particular, in the center region, many fine grains are almost produced directly by various twinning induced segmentation of the lattices. The dislocation density both in the twinned and other areas is relatively high, which can be inferred directly from the KAM map shown in Fig.5c. So, it can be speculated that besides the fine twinning segments, other fine gains or sub-grains are mainly produced through dislocations rearrangement. The speculation will be further verified through TEM observation in the following section.

From the observations presented in Fig.4 and Fig.5, it can be informed that the twinning behavior at the nano-scale is more complex. Besides the co-existence of $\{10\bar{1}1\}$ and $\{10\bar{1}3\}$ compression twins as mentioned above, the $\{10\bar{1}2\}$ extension twins are mainly activated as secondary twinning model and nucleate at different sites of the $\{10\bar{1}1\}$ twin

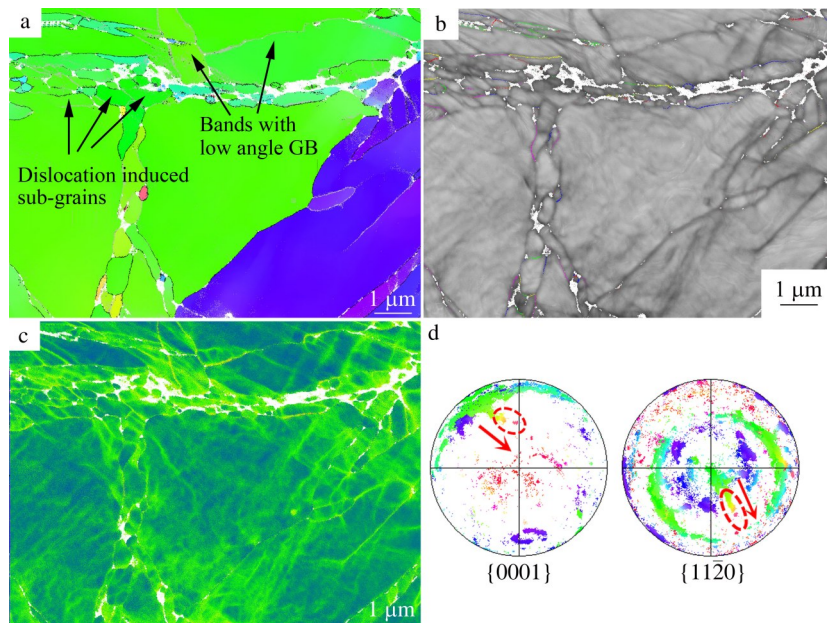


Fig.4 TKD IPF map (a), corresponding Kikuchi band contrast map (b), KAM map (c), $\{0001\}$ and $\{1120\}$ pole figures (d) of the as-rolled alloy (standard IPF and colors for representative twin boundary variants are the same as Fig.1)

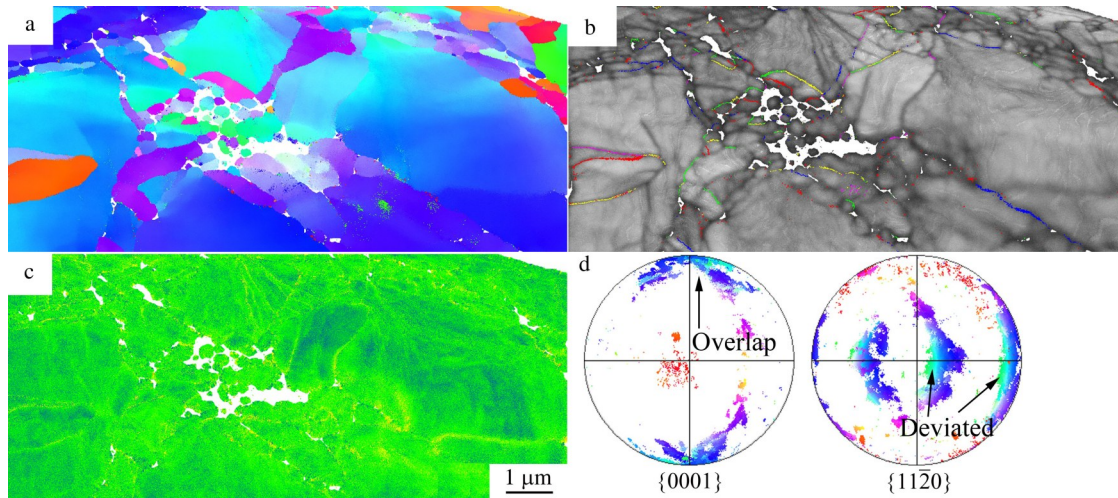


Fig.5 TKD IPF map (a), Kikuchi band contrast map (b), KAM map (c), $\{0001\}$ and $\{11\bar{2}0\}$ pole figures (d) of as-rolled alloy (standard IPF and colors for representative twin boundary variants are the same as Fig.1)

segments almost simultaneously, which is different from the EBSD observations detected at a larger step size. The secondary twinning accompanied by dynamic recrystallization within the recrystallized areas reveals that the multiple twinning deformation not only can accommodate the local plastic strain, but also plays a critical role in dividing the lattices within these areas that can accelerate dynamic recrystallization via a unique way. Yet the dominated twin types are still $\{10\bar{1}1\}$ - $\{10\bar{1}2\}$ double twin and $\{10\bar{1}1\}$ compression twin, consistent with the EBSD observations.

2.3 Effect of dislocation activity on grain refinement

From the observations it can be seen that during large strain hot rolling, twinning deformation plays an important role in the internal stress relieving; it is conducted not only through twinning deformation itself, but also via lattice reorientation and dynamic lattice fragmentation to trigger more favorable dislocation activities, especially the latter one which governs the whole microstructural evolution. Because dislocation slip is still the primary contributor to plastic strain, the core of twinning deformation for plasticity lies in avoiding stress concentration on unfavorable planes for basal slip^[28] and the slip-twin interactions^[29]. So the dislocation activity is non-negligible.

Fig. 4d and Fig. 5d exhibit the micro-texture distribution corresponding to the TKD data presented in Fig.4a and Fig.5a, respectively, from which the related deformation mechanism in grains can be deduced from a more macroscopic perspective. The $\{0001\}$ and $\{11\bar{2}0\}$ pole figures as shown in Fig.4d show a continuous fiber micro-texture and the basal planes spread around a common $\langle 11\bar{2}0 \rangle$ rotation axis, which mainly originates from the large grain (green color in the IPF map of Fig. 4a). The continuous orientation distribution in large grain reveals a mutual coordination between the deformation twinning and basal slips, because basal dislocation slips can also produce a rotation of the lattices around the $\langle 11\bar{2}0 \rangle$ axis^[30]. For some fine grains or sub-grains

in the vertical band, their orientation deviates from the fiber micro-texture but still show a continuity (as indicated by the red circles, and the arrows shows their deviation direction), which indicates the participation of other dislocation slip systems beyond the dominated basal dislocation slips. While the orientation distribution in the small grain (blue color in the IPF map of Fig.4a) is more scattered and the grain orientation is separated into several segments by the twins, deformation bands and dynamic recrystallized grains. In Fig.5d, the micro-texture shows the orientation distribution of one grain that undergoes dynamic recrystallization, and it can be seen that the major orientation (blue and bluish colors) concentrates at the top and bottom poles of the $\{0001\}$ pole figure, exhibiting a basal-like micro-texture. While the orientation of twinned and some recrystallized areas tends to extend the basal-like micro-texture into a fiber micro-texture, and the reason is the same as that indicated in Fig. 4d. Moreover, the orientations correspond to blue and bluish colors are nearly overlapped in the $\{0001\}$ pole figure, but the bluish color clearly deviates from the blue color in the $\{11\bar{2}0\}$ pole figure, which reveals the intense prismatic slips in the bluish color areas of the IPF map (Fig. 5a) that are separated from the dominated orientation of the grain (i.e., the blue color) around the c -axis.

The TEM images presented in Fig.6 clearly exhibit the slip-twin interactions, dislocation-induced nano grains, and dislocation cells. Fig. 6a reveals a disunited $\{10\bar{1}1\}$ compression twin, the left part of which keeps a unity along the thickness of twin lamella, while moving to the right the uneven dislocation activities divide the unity into several segments. The dislocation tangles can be clearly seen in some regions. Fig. 6b shows two adjoining nano grains that are separated from each other through a common $\langle 01\bar{1}1 \rangle$ axis rotation, forming a low angle grain boundary between them. It is evident that both basal and non-basal slips participate in this process. The dynamically recrystallized nano grains/sub-grains as well as dislocation cells shown in Fig.6c and 6d further prove the intense dislocation activity, consistent with

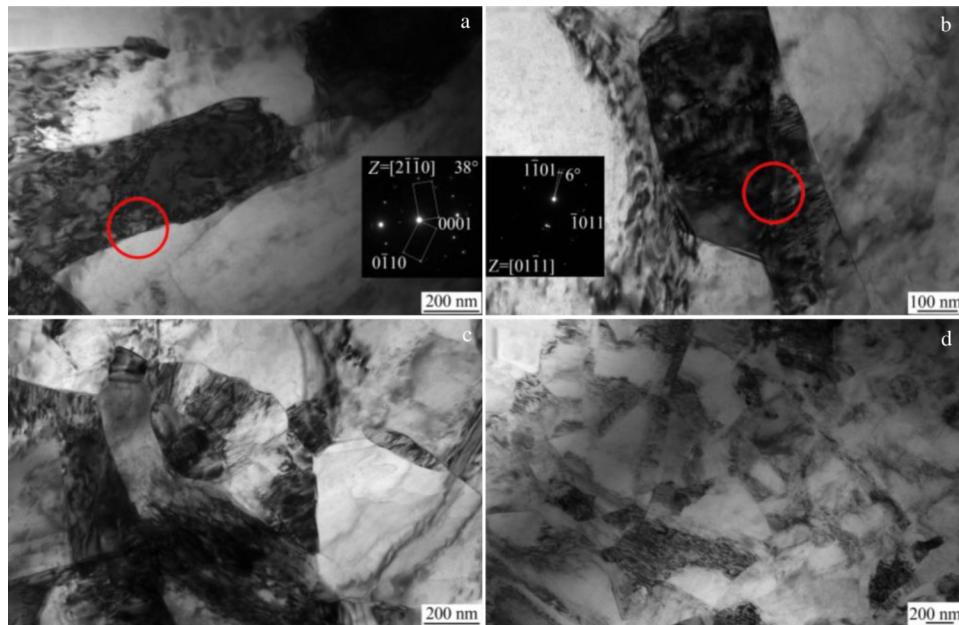


Fig.6 TEM images of $\{10\bar{1}1\}$ compression twin that has been fragmented by uneven dislocation activities in it (a), two adjoining nano grains with a low misorientation angle of 6° (b), and dynamically recrystallized nano grains and dislocation cells (c, d)

the TKD results shown in Fig. 4 and Fig. 5. In summary, dislocation activity facilitates dynamic recrystallization within the twinned area and successfully extends the process to the matrix. It greatly enables the uniform deformation of alloy during large strain hot rolling processing. The dislocation slips and multiple twinning deformation mutually coordinate the whole microstructure evolution of the alloy, and both of them enable the formability of alloy sheet.

3 Conclusions

1) The pre-extruded Mg-3Y alloy exhibits a recrystallized equiaxial grain structure with an average grain size of $45 \mu\text{m}$, and the weak texture with the tilted basal poles is apart from the sheet normal direction.

2) During large strain hot rolling processing, multiple deformation twinning types, especially the $\{10\bar{1}1\}$ compression twinning and $\{10\bar{1}1\} - \{10\bar{1}2\}$ double twinning play an important role in plastic strain accommodation. And these twins produce extensively distributed narrow bands across the deformed grains.

3) Dynamic recrystallization occurs within the band structure due to the high dislocation density, and spreads to non-twinned regions simultaneously, which enables the uniform plastic deformation during hot rolling processing. Moreover, the $\{10\bar{1}2\}$ secondary twinning also plays the role of dividing the lattices within dynamic recrystallization areas that turn to accelerate the recrystallization process via a unique way.

4) Micro-texture analysis and TEM observation of deformed regions reveal that dislocation slips are still the dominated contributor to plastic strain during large strain hot rolling processing. Dislocation slips and multiple twinning deformation mutually coordinate the formability of the alloy sheet.

References

- 1 Wu Zhaoxuan, Ahmad Rasool, Yin Binglun *et al. Science*[J], 2018, 359: 447
- 2 Edwin Eyram Klu, Jiang Jinghua, Bassiouny Saleh *et al. Rare Metal Materials and Engineering*[J], 2022, 51(2): 491
- 3 Wang Ziyi, Chen Xianhua, Shu Yankai *et al. Rare Metal Materials and Engineering*[J], 2022, 51(9): 3138
- 4 Ravaji Babak, Joshi Shailendra P. *Acta Materialia*[J], 2021, 208: 116 743
- 5 Indurkar Padmeya P, Baweja Shahmeer, Perez Robert *et al. International Journal of Plasticity*[J], 2020, 132: 102 762
- 6 Mishra Sourav, Khan F, Panigrahi S K. *Journal of Magnesium and Alloys*[J], 2022, 10(9): 2546
- 7 Wu Huajie, Zhong Feng, Wu Ruizhi *et al. Materials Science and Engineering A*[J], 2022, 859: 144 199
- 8 Stanford N, Barnett M R. *Materials Science and Engineering A*[J], 2008, 496(1–2): 399
- 9 Pei Risheng, Zou Yongchun, Zubair Muhammad *et al. Acta Materialia*[J], 2022, 233: 117 990
- 10 Liu Ke, Liang Jingtao, Du Wenbo *et al. Rare Metals*[J], 2021, 40(8): 2179
- 11 Wang Lisha, Jiang Jinghua, Saleh Bassiouny *et al. Acta Metallurgica Sinica*[J], 2020, 33(9): 1180
- 12 Liu Huan, Ju Jia, Lu Fumin *et al. Materials Science and Engineering A*[J], 2017, 682: 255
- 13 Fadaei Abbas, Farahafshan Faramarz, Sepahi-Boroujeni Saeid. *Materials & Design*[J], 2017, 113: 361
- 14 Azzeddine Hiba, Bradai Djamel, Baudin Thierry *et al. Progress in Materials Science*[J], 2022, 125: 100 886

- 15 Wang Tianzi, Zheng Haipeng, Wu Ruizhi et al. *Advanced Engineering Materials*[J], 2016, 18(2): 304
- 16 Luo Dan, Wang Huiyuan, Zhao Liguang et al. *Materials Characterization*[J], 2017, 124: 223
- 17 Li Xinyu, Xia Weijun, Chen Jihua et al. *Transactions Nonferrous Metals Society of China*[J], 2021, 31(10): 2885
- 18 Guo Fei, Zhang Dingfei, Fan Xiaowei et al. *Journal of Alloys and Compounds*[J], 2016, 663: 140
- 19 Wang Kui, Wang Jingfeng, Peng Xing et al. *Materials Science and Engineering A*[J], 2019, 748: 100
- 20 Ventura Nicolò M Della, Kalácska Szilvia, Casari Daniele et al. *Materials & Design*[J], 2021, 197: 109 206
- 21 Lu S H, Wu D, Chen R S, Han En-Hou. *Materials & Design*[J], 2020, 191: 108 600
- 22 Basu I, Al-Samman T. *Acta Materialia*[J], 2015, 96: 111
- 23 Zhu S Q, Ringer Simon P. *Acta Materialia*[J], 2018, 144: 365
- 24 Niknejad Seyedtirdad, Esmaceli Shahrzad, Zhou Norman Y et al. *Acta Materialia*[J], 2016, 102: 1
- 25 Yoo M H. *Metallurgical Transactions A*[J], 1981, 12: 409
- 26 Kumar M Arul, Gong M, Beyerlein I J, Wang J et al. *Acta Materialia*[J], 2019, 168: 353
- 27 Sun Q, Zhang X Y, Yin R S et al. *Scripta Materialia*[J] 2015, 108: 109
- 28 Zhao Shiteng, Zhang Ruopeng, Chong Yan et al. *Nature Materials*[J], 2021, 20: 468
- 29 Molodov Konstantin D, Al-Samman Talal, Molodov Dmitri A. *Acta Materialia*[J], 2017, 124: 397
- 30 Molodov Konstantin D, Al-Samman Talal, Molodov Dmitri A et al. *Acta Materialia*[J], 2014, 76: 314

Mg-3Y 合金大应变量轧制过程中的孪生辅助动态再结晶及组织演变

陈毓美, 刘权震, 刘安国, 侯秀丽

(江苏大学 材料科学与工程学院, 江苏 镇江 212013)

摘要: 采用预挤压加单道次大应变量热轧制的方法制备了 Mg-3Y (质量分数, %) 合金板材。并研究了大应变量轧制过程中不同孪晶类型对合金动态再结晶 (DRX) 及组织演变的影响。结果表明, 在挤压比为 8:1 的预挤压过程中, 合金内部发生了几乎完全的动态再结晶。而在接下来的大应变量热轧制过程中, 孪生变形尤其是 $\{10\bar{1}1\}$ 压缩孪晶及 $\{10\bar{1}1\}$ - $\{10\bar{1}2\}$ 双孪晶在协调合金的塑性应变中发挥了重要作用。此外, 大量动态再结晶在压缩孪晶及双孪晶内部发生, 并扩展到非孪晶区域, 有效缓解了轧制过程中的内应力集中。上述 2 个过程对提高合金在大应变量轧制中的成形性均起到了促进作用。

关键词: 镁合金; 稀土; 大应变量轧制; 孪生; 动态再结晶

作者简介: 陈毓美, 女, 1997 年生, 江苏大学材料科学与工程学院, 江苏 镇江 212013, 电话: 0511-88797887, E-mail: 1623208587@qq.com